Photoinduced Electron Transfer in Porphyrin- and Fullerene/Porphyrin-Based Rotaxanes as Studied by Time-Resolved EPR Spectroscopy

Manuela Jakob,[†] Alexander Berg,[†] Roy Rubin,[†] Haim Levanon,*[,†] Ke Li,[‡] and David I. Schuster[‡]

Department of Physical Chemistry, Hebrew University of Jerusalem, Jerusalem 91904, Israel, and Department of Chemistry, New York University, New York, New York 10003

Received: January 13, 2009; Revised Manuscript Received: March 23, 2009

Photoinduced intramolecular electron-transfer (ET) and energy-transfer (EnT) processes in two rotaxanes, one containing both zinc porphyrin and C_{60} fullerene moieties incorporated around the Cu(I) bisphenanthroline core [$(ZnP)_2-Cu(I)(phen)_2-C_{60}$] and a second complex lacking the fullerene [$(ZnP)_2-Cu(I)(phen)_2$], were studied by time-resolved electron paramagnetic resonance (TREPR) spectroscopy at 9.5 GHz (X-band) combined with a selective photoexcitation of the rotaxane moieties. The experiments were carried out in isotropic toluene and ethanol and in anisotropic nematic liquid-crystal (E-7) media over a wide range of temperatures corresponding to the different states of the solvents. The TREPR results are compared with those obtained previously by optical methods in dichloromethane at room temperature. It is demonstrated that the efficiencies and pathways of the light-driven ET and EnT processes in both rotaxanes strongly depend on the properties of their microenvironment, resulting in the formation of distinct charge-separated states under different experimental conditions. The complementary results revealed by the optical and TREPR techniques are attributed to the relatively high conformational mobility of the mechanically interlocked rotaxane systems. Because of the solute−solvent interactions, the rotaxanes are able to change conformation in different microenvironments, which affects the parameters of the photoinduced processes occurring in these systems.

Introduction

Since the discovery of long-range photoinduced electron transfer (ET) in photosynthesis,[1] one of the most debated problems is the question of how such ET events proceed through various noncovalently linked protein pathways.[2] It is well-established that the chromophores in the native reaction centers are highly organized by the protein environment, providing the necessary electronic coupling between the electron donors and acceptors for efficient intra- and intermolecular ET.[2] Understanding the mechanisms of biological ET reactions is critical in developing supramolecular assemblies that can serve as materials for solar energy conversion and molecular electronics applications.

The complexity of the in vivo apparatus prompts the search for relatively simple arrays that can mimic the major processes and states occurring in photosynthetic reaction centers.[3,4] In this context, rotaxanes, which are supramolecules composed of one or more macrocycles encircling one or more linear components terminated by bulky stoppers,[5] are promising systems. This is due to their mechanically interlocked electron donor and electron acceptor arranged at relatively fixed positions without any direct covalent linkage. Therefore, the rotaxane entities often have a high freedom of mobility, which can result in photoinduced large-amplitude conformational changes, similar to those occurring in the native apparatus.[6−11] Moreover, the topology of rotaxanes prevents a close approach of the donor to the acceptor, so that intramolecular electronic coupling, following photoexcitation, must take place through the specially designed spacer. Thus, by choosing the spacer molecule, one can strongly affect the rates of forward and backward ET.[12]

In recent years, these special features have attracted considerable interest in photoactive rotaxanes that faithfully mimic ET and energy-transfer (EnT) processes that take place in natural photosynthesis.[13,14] The light-driven ET in rotaxanes can also serve as a driving force for achieving light-controlled translational or conformational motion of their components, which can be used to construct molecular machines and molecular motors.[6,13,15−20] Advantages such as direct energy input and reversibility of ET processes that allow repetition of the operation at will, along with convenient time scale of the cycle, make photoactive rotaxanes particularly promising in this regard.[21] Moreover, the temporal characteristics of the molecular motor operations in rotaxanes can be controlled by choosing various feasible ET pathways having different charge separation and charge recombination rates.[14,22,23] Detailed investigation of the dynamics and kinetics of light-driven processes in rotaxanes provides the possibility of establishing structure−function relationships in these supramolecules. Obviously, gaining control over such molecular motion is a crucial step toward creating novel "smart" molecules that can perform specific functions.

Among biomimetic systems with rotaxane architectures, porphyrin−fullerene complexes are particularly attractive because of the excellent electron-donor properties of porphyrins and the unique electron-acceptor properties of fullerenes.[9−11,24]

This work presents an X-band (9.5 GHz) time-resolved electron paramagnetic resonance (TREPR) study of the light-driven intramolecular ET processes in two rotaxanes, the first of which contains two Zn tetraarylporphyrin (ZnP) moieties and a Cu(I) bisphenanthroline [$Cu(I)(phen)_2$] complex [$(ZnP)_2-Cu(I)(phen)_2$] (Figure 1a) and the second of which incorporates two Zn tetraarylporphyrins (ZnP) and one C_{60} moiety around

* E-mail: levanon@chem.ch.huji.ac.il.
[†] Hebrew University of Jerusalem.
[‡] New York University.

10.1021/jp900331j CCC: $40.75
Published on Web 04/29/2009

the central Cu(I) bisphenanthroline [Cu(I)(phen)$_2$] core [(ZnP)$_2$−Cu(I)(phen)$_2$−C$_{60}$] (Figure 1b). These systems were studied recently by optical methods in dichloromethane (DCM) at room temperature; in addition, the various processes that occurred following photoexcitation were studied, and intermediate states were characterized.[24−26] The present experimental approach extends the information obtained in a previous optical investigation. TREPR experiments were performed in frozen toluene and ethanol, as well as in different phases of a nematic liquid crystal (LC), E-7. The high sensitivity, spectral and time resolution of EPR spectroscopy, combined with the use of an LC as solvent, enable transient paramagnetic species in the system of interest to be followed in real time. Analysis of the TREPR spectra under different experimental conditions provides additional information that cannot be derived from optical studies of the dynamic, kinetic, and magnetic parameters associated with the ET precursors and intermediates. Thus, TREPR spectroscopy, which allows experiments over a wide range of solvents, temperatures, and time intervals, successfully complements optical spectroscopy in revealing the mechanisms associated with electron-transfer processes.[21,27−31]

Experimental Section

LC (E-7, Merck Ltd.) was used without further purification. Toluene (ACS reagent, J.T. Baker Inc.) was dried and kept under vacuum during sample preparation. Ethanol (Chromasolv, absolute, HPLC grade, Sigma-Aldrich) was used without further purification. The phase transitions of E-7, toluene, and ethanol are as follows

$$\begin{aligned}
&\text{E-7:} \quad \text{crystalline} \overset{210\ \text{K}}{\longleftrightarrow} \text{soft crystalline} \overset{263\ \text{K}}{\longleftrightarrow} \\
&\qquad\qquad \text{nematic} \overset{333\ \text{K}}{\longleftrightarrow} \text{isotropic} \\
&\text{toluene:} \quad \text{glass} \overset{117\ \text{K}}{\longleftrightarrow} \text{amorphous} \overset{178\ \text{K}}{\longleftrightarrow} \text{liquid} \\
&\text{ethanol:} \quad \text{glass} \overset{97\ \text{K}}{\longleftrightarrow} \text{amorphous} \overset{156\ \text{K}}{\longleftrightarrow} \text{liquid}
\end{aligned} \tag{1}$$

Procedures for the synthesis of the rotaxanes used in this study are described elsewhere.[24−26] The rotaxanes were first dissolved in toluene ($\sim 5 \times 10^{-4}$ M), which was then evaporated, and the LC was introduced into the pyrex tube. The samples were degassed by several freeze−pump−thaw cycles on a vacuum line and sealed under a vacuum.

X-band TREPR experiments (response time of 150−200 ns) were performed in degassed 4-mm-o.d. pyrex tubes employing a Bruker ESP 380 EPR spectrometer with field modulation disconnected.[32] The EPR signals were taken from the microwave preamplifier and transferred to a Le Croy 9400 digital oscilloscope after being passed through a low-noise filter and amplified by a fast amplifier (10 dB). A frequency counter (EIP, model 545) was used to monitor the microwave frequency. The magnetic field was controlled using a precision NMR Teslameter PT 2025 instrument (Metrolab). Estimation of the g factors was performed by employing DPPH free radical ($g = 2.0036$) (Aldrich Chemical Co., Inc.). Transient traces of the EPR signals were acquired and accumulated on a PC through a GPIB interface. The spectra at different time windows after the laser pulse were reconstructed from the full set of data obtained over a chosen scan range of the magnetic field. The temperature was

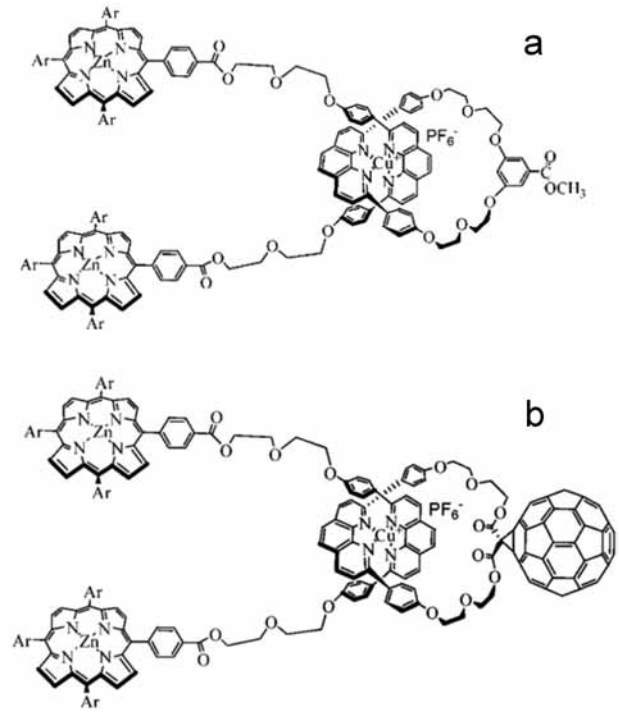

Figure 1. Chemical structures of the rotaxane molecules: (a) (ZnP)$_2$−Cu(I)(phen)$_2$, (b) (ZnP)$_2$−Cu(I)(phen)$_2$−C$_{60}$.

controlled by a Bruker variable-temperature unit (model ER411 VT). The samples were illuminated by an optical parametric oscillator (OPO; Panther III, Continuum Corp.) pumped by the third harmonic (355 nm) of a Nd:Yag laser (Surelite II, Continuum Corp.): 10 mJ/pulse OPO output, 10 Hz repetition rate, and 10 ns pulse duration. Several control experiments were performed with a Q-band (34 GHz) EPR spectrometer as described elsewhere.[33]

The orientation of the LC director, **L**, with respect to the magnetic field, **B**, is determined by the sign of the anisotropy of the diamagnetic susceptibility, $\Delta\chi$ ($\Delta\chi = \chi_{\parallel} - \chi_{\perp}$).[34] Because $\Delta\chi$ is positive for E-7, the default orientation in the nematic phase is $\mathbf{L} \parallel \mathbf{B}$. Rotation of the frozen sample by 90° about an axis perpendicular to the external magnetic field yields the director orientation $\mathbf{L} \perp \mathbf{B}$. Analysis of the TREPR line shapes was performed as described elsewhere.[35,36]

The radical-pair (RP) spectra were analyzed in terms of spin-correlated-radical-pair (SCRP)[37,38] and triplet-radical-pair (TRP) mechanisms.[39] The SCRP spectra consist of two antiphase doublets, centered at the g factors of the individual radicals of the pair. The splitting of each doublet is determined by the spin−spin exchange interaction integral, J, and the zero-field splitting (ZFS) parameter D. The experimentally observed spectrum is a superposition of the four-line spectra for all possible orientations of the RP with respect to the external magnetic field, **B**. The positions (ω_{ij}) of the four EPR transitions for CRP are given by[37,38,40]

$$\begin{aligned}
\omega_{12} &= \omega_0 - \Omega - J + D_{zz} \\
\omega_{34} &= \omega_0 - \Omega + J - D_{zz} \\
\omega_{13} &= \omega_0 + \Omega - J + D_{zz} \\
\omega_{24} &= \omega_0 + \Omega + J - D_{zz}
\end{aligned} \tag{2}$$

where

$$\omega_0 = \beta B_0(g_1 + g_2)/\hbar$$
$$\Omega^2 = (J + D_{zz}/2)^2 + Q^2$$
$$Q = \frac{1}{2}(g_1 - g_2)\mu\hbar^{-1}B_0 + \frac{1}{2}\left(\sum_i a_{1i}m_{1i} - \sum_j a_{2j}m_{2j}\right) \quad (3)$$
$$D_{zz} = D[\cos^2(\xi) - 1/3]$$

where $g_{1,2}$ and $m_{1,2i}$ are the g factors and hyperfine constants for radicals 1 and 2, respectively, and ξ is the angle between the dipolar axis and the magnetic field direction, **B**. The EPR signal phase is determined by the SCRP sign rule[37,38]

$$\Gamma = -\mu \times \text{sign}\{J + D[3\cos^2(\xi) - 1]\} = \begin{cases} - \text{ e,a} \\ + \text{ a,e} \end{cases} \quad (4)$$

where μ is -1 or $+1$ for a singlet or a triplet precursor, respectively.

In all EPR experiments, the spectra did not show any saturation effects over a wide microwave power range (15−93 mW), and the corresponding kinetics did not exhibit any oscillations, satisfying underdamping conditions.[41]

The distances between the supramolecular entities were calculated using HyperChem modeling, which allows for the computation of the minimum-energy molecular geometry in a vacuum. Thus, in the condensed media, the determined spacing of the rotaxane parts can be considered as estimations.

Results

We first present the main photophysical parameters of the two rotaxanes studied here (Figure 1a,b). Because the quenching routes of the photoexcited states of the chromophore depend on their microenvironment,[42] TREPR experiments were performed in nonpolar (toluene, dielectric constant $\varepsilon = 2.38$)[43] and polar (ethanol, $\varepsilon = 25.3$)[43] isotropic solvents and in the anisotropic LC E-7 ($\varepsilon_{\parallel} = 19.0$, $\varepsilon_{\perp} = 6.2$)[44] over a wide range of temperatures.[45] Samples were excited selectively at 460 and 532 nm. At 460 nm, the absorption of the Cu(I)(phen)$_2$ moiety is maximal ($\kappa \approx 1700$ cm^{-1} M^{-1}),[46] whereas the absorption of ZnP is minimal ($\kappa \approx 1550$ cm^{-1} M^{-1}).[47] On the other hand, at 532 nm, Cu(I)(phen)$_2$ absorption is low ($\kappa \approx 270$ cm^{-1} M^{-1}), whereas ZnP absorption is high ($\kappa \approx 8150$ cm^{-1} M^{-1}).[47] The extinction coefficients of C_{60} at 460 and 532 nm were found to be 200 and 840 cm^{-1} M^{-1}, respectively.[48,49] Thus, the probabilities of absorption of the 460-nm light by the (ZnP)$_2$, Cu(I)(phen)$_2$, and C_{60} entities in the rotaxane correspond to the ratio of their extinction coefficients, namely, 1.8:1:0.1 at 460 nm and 60:1:3 at 532 nm. Therefore, upon 460-nm excitation of (ZnP)$_2$−Cu(I)(phen)$_2$, the rotaxane with photoexcited ZnP and Cu(phen)$_2$ entities should be obtained initially with comparable probabilities, whereas upon excitation at 532 nm, the photoexcited porphyrin entity will dominate. In the case of (ZnP)$_2$−Cu(I)(phen)$_2$−C_{60}, ZnP and Cu(I)(phen)$_2$ electronic excited states will be generated upon irradiation at 460 nm, prevailing over excited C_{60}, whereas most of the photons at 532 nm will be absorbed by ZnP (predominantly) and C_{60} (to a lesser extent) as compared to Cu(I)(phen)$_2$.

The singlet and triplet excited-states energies, respectively, of the rotaxane constituents are as follows: ZnP, 2.12 and 1.59 eV;[50] Cu(I)(phen)$_2$, 1.91 and 1.73 eV (averaged);[51,52] and C_{60}, 1.80 and 1.57 eV.[50] Here, it should be noted that these values were determined in the liquid isotropic solvents and might change slightly under our experimental conditions, so they were used only as estimations. Unfortunately, the corresponding precise values in the frozen isotropic solvents and LC matrixes are not available.

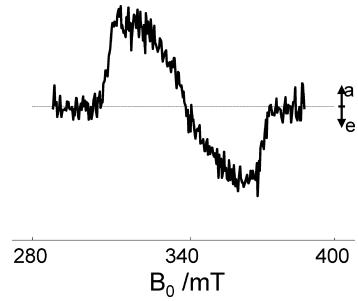

Figure 2. TREPR spectrum [$\chi''(B_0)$ presentation] of (ZnP)$_2$−Cu(I)(phen)$_2$ in toluene at 170 K. Spectrum was recorded 1.2 μs after laser-pulse photoexcitation at 460 nm.

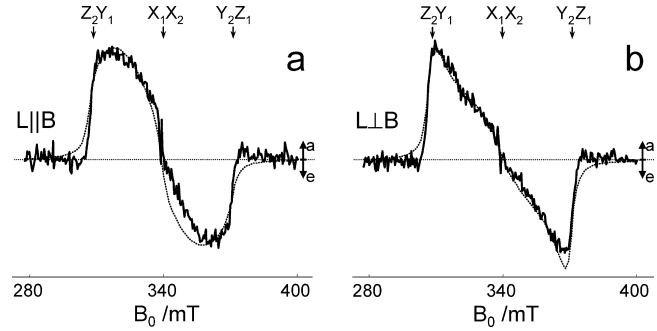

Figure 3. TREPR spectra [$\chi''(B_0)$ presentation] of (ZnP)$_2$−Cu(I)(phen)$_2$ in E-7 at 170 K for **L** || **B** and **L** ⊥ **B** orientations. Spectra were recorded 0.96 μs after laser-pulse photoexcitation at 460 nm. Dotted curves superimposed on the experimental spectra are computer simulations with the parameters given in Table 1.

(ZnP)$_2$−Cu(I)(phen)$_2$. ***Isotropic Solvents.*** Photoexcitation of (ZnP)$_2$−Cu(I)(phen)$_2$ at 460 and 532 nm in frozen toluene and ethanol gives rise to practically identical polarized triplet spectra that exhibit absorption, emission (a,e) electron spin polarization (ESP) patterns with a spectral width of ∼70 mT. Figure 2 presents the TREPR spectrum of (ZnP)$_2$−Cu(I)(phen)$_2$ in toluene at 170 K following 460-nm photoexcitation. A similar spectrum, but with a lower signal-to-noise ratio, was obtained in frozen ethanol (not shown).

Liquid Crystal. Photoexcitation at 460 and 532 nm of (ZnP)$_2$−Cu(I)(phen)$_2$ in the crystalline phase of E-7 (eq 1) was carried out in two orientations, **L** || **B** and **L** ⊥ **B**. TREPR spectra (at 460 nm, 170 K) are presented in Figure 3. In both **L** || **B** and **L** ⊥ **B** orientations, the spectra exhibit two signals, a broad one (∼70 mT width) with a,e polarization pattern and, superimposed, a narrow line ($H_{pp} \approx 0.7$ mT). When the sample orientation is changed from **L** || **B** to **L** ⊥ **B**, the narrow spectrum reverses its polarization pattern from e,a to a,e. The g values of the broad and narrow signals are calculated to be ∼2.00 and ∼2.0041, respectively. Furthermore, the ESP patterns of the two signals at both orientations do not change in time. It should be noted that at 113 and 140 K, the narrow signal was not observed, whereas the broad one remained intact. In the soft crystalline (Figure 4) and nematic (not shown) phases of E-7, the narrow e,a signal reverses its phase to a,e at later times. It should be noted that at higher temperatures, in the soft crystalline and nematic phases, the perpendicular orientation cannot be achieved because of the fast realignment of the chromophore to the parallel orientation.[53]

Computer simulations of the broad spectra provided the ZFS parameters of the paramagnetic species, as well as relative population rates of its triplet sublevels. These data are presented in Table 1, together with the corresponding parameters of the model porphyrin (ZnTPP) recorded under the same experimental

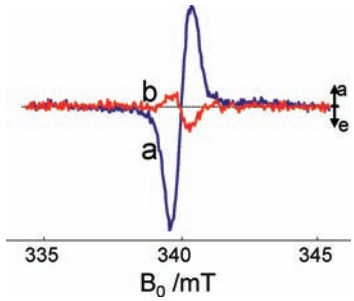

Figure 4. Time evolution of the narrow signal observed in photoexcited $(ZnP)_2-Cu(I)(phen)_2$ in E-7 at 240 K. Spectra [$\chi''(B_0)$ presentation] were recorded (a) 0.8 and (b) 2.0 μs after laser-pulse photoexcitation at 460 nm.

conditions.[54] The close similarities of these parameters show that the observed broad spectra can be ascribed to the lowest triplet excited state of the porphyrin entity (^{3}ZnP*), in $(ZnP)_2-Cu(I)(phen)_2$. The difference between the *E* values of the ZnP entity and pristine ZnTPP in ethanol (Table 1) probably can be attributed to differences in their molecular structures and symmetries.[55,56]

Photoexcitation of this compound in the crystalline phase at 532 nm in the **L** || **B** and **L** ⊥ **B** orientations results only in broad spectra that are essentially identical to those observed after 460-nm excitation. Upon 532-nm photoxcitation, the narrow signal appears in neither the soft crystalline nor the nematic phase of E-7.

$(ZnP)_2-Cu(I)(phen)_2-C_{60}$. ***Isotropic Solvents.*** Photoexcitation of rotaxane $(ZnP)_2-Cu(I)(phen)_2-C_{60}$ at 460 and 532 nm gives rise to three overlapping a,e signals, one broad signal of ~70 mT width assigned to ^{3}ZnP* and two narrower signals with $H_{pp} \approx 9.4$ and 4.2 mT, all with *g* values of ~2.00, which were observed in early times in both solvents over a wide temperature range (124−190 K in toluene and 124−160 K in ethanol). Figure 5 presents the TREPR spectrum of this compound in toluene at 140 K after 460-nm photoexcitation. A similar spectrum, but with a lower signal-to-noise ratio, was obtained in frozen ethanol (not shown). Control Q-band (34 GHz) EPR experiments with higher time resolution (in toluene at 140 K, using 532-nm excitation) showed that the narrow signal appeared 100 ns after the laser pulse, whereas the broad signal became visible ~160 ns after the laser pulse. At later times, the signals also behaved differently. The broad signal displayed the usual decay, whereas the narrow one reversed its polarization pattern to e,a and then decayed during tens of microseconds. In toluene glass[57] (at 102 K), only the broad a,e signal was observed, and it retained its polarization pattern with time. The temperature of the ethanol glass transition (~97 K)[58] was unattainable in our experiments.

Liquid Crystal. Excitation of $(ZnP)_2-Cu(I)(phen)_2-C_{60}$ at 460 nm in the crystalline phase (at least down to 120 K) for **L** || **B** results in three signals of different widths, namely, an a,e signal of 70 mT, an a,e signal of 20 mT, and an e,a signal with $H_{pp} \approx 0.7$ mT (Figure 6a,c). Upon rotation of the sample by 90° to **L** ⊥ **B**, the first two signals remain unchanged, whereas the third reverses its phase from e,a to a,e (Figure 6b,d). Furthermore, none of the observed spectra change their polarization patterns with time.

In the soft crystalline (Figure 7) and nematic (not shown) phases, irradiation at 460 nm results in three signals that are similar to those obtained in the crystalline phase at this excitation wavelength. The sole exception was the change of the narrow signal pattern from e,a to a,e with time (Figure 7).

Excitation of the sample at 532 nm under the same experimental conditions (120−293 K, at both sample orientations in the crystalline phase of LC), gives rise to the first two broad signals mentioned above, but the narrow signal is not observed. The detected signals conserve their polarization patterns with time and with change in orientation.

Discussion

$(ZnP)_2-Cu(I)(phen)_2$. ***Isotropic Solvents.*** Under the same experimental conditions, the TREPR spectra of $(ZnP)_2-Cu(I)(phen)_2$ are very similar to those of ZnTPP (Table 1).[54,56] This finding indicates that the obtained rotaxane spectra can be attributed to the ^{3}ZnP*. This observation can be explained as follows: In $(ZnP)_2-Cu(I)(phen)_2$, the probability of 460-nm light absorption by the zinc porphyrin entity is 1.8 times higher than that of the copper phenanthroline complex. Thus, irradiation at 460 nm should produce comparable amounts of excited ZnP and $Cu(I)(phen)_2$ moieties. It was shown previously that photoexcitation of the $Cu(I)(phen)_2$ complex in solution results in the formation of a metal-to-ligand charge-transfer (MLCT) state, which is efficiently quenched by the porphyrin entity to give ^{3}ZnP*.[24,26] The short lifetime of the MLCT state (~5 ns)[25] prevents it from being detected in our experiments. On the other hand, 460-nm excitation of ZnP causes the efficient formation of its long-lived triplet excited state.[24−26] Thus, the TREPR spectrum of $(ZnP)_2-Cu(I)(phen)_2$ in both isotropic solvents exhibits only the lower triplet state of the ZnP moiety without the contribution of any other paramagnetic species (see Figure 2). Upon photoexcitation at 532 nm, where the probability of light absorption by ZnP is ~60 times higher than that of $Cu(I)(phen)_2$, the observation of only ^{3}ZnP* in the spectra of $(ZnP)_2-Cu(I)(phen)_2$ is to be expected.

An earlier optical study of this system in DCM at room temperature showed only the occurrence of exergonic EnT processes, leading eventually to ^{3}ZnP*, without the formation of any charge-separated states.[24−26]

Liquid Crystal. As established above, the narrow signal observed upon 460-nm excitation of $(ZnP)_2-Cu(I)(phen)_2$ cannot be attributed to the photoexcited triplet state of the ZnP or $Cu(I)(phen)_2$ entities. Observation of the phase inversion of the signal upon 90° rotation of the sample allows this signal to be assigned to the weakly coupled SCRP. This assignment is based on SCRP theory of a weakly coupled RP.[37,38,59,60] For such pairs, a derivative-like signal is predicted for the X-band EPR spectrum whose phase pattern, absorption or emission, should depend on the molecular orientation of the RP with respect to the magnetic field.[37,38,59] Thus, when the RP molecular orientation was changed by 90°, it was indeed observed that the phase pattern changed from e,a to a,e (Figure 3), which is typical for the SCRP case. In addition, SCRP mechanism theory explicitly reveals the precursor state multiplicity of the electron donor from the polarization pattern of the RP spectrum. Taking into account the e,a polarization pattern of the narrow signal and employing expression 4, one can conclude that the precursor of the observed SCRP is a singlet excited state. Furthermore, a phase inversion of the time-evolved SCRP spectrum usually indicates the participation of two ET routes in the formation of the RP, that is, a singlet-initiated SCRP accompanied by a triplet-initiated pathway[32,61,62] as it follows from the SCRP sign rule (expression 4). To determine the SCRP constituents, we need to consider the possible ET routes on photoinduced $(ZnP)_2-Cu(I)(phen)_2$ at 460 nm, where the probabilities of light absorption by the ZnP and $Cu(I)(phen)_2$ entities are comparable. It was shown earlier for $(ZnP)_2-Cu(I)(phen)_2$ that involvement

TABLE 1: Magnetic Parameters of Rotaxane Constituents and Corresponding Pristine Compounds

molecule	moiety	solvent	T (K)	D^a ($\times 10^4$ cm^{-1})	E^a ($\times 10^4$ cm^{-1})	A_x:A_y:A_z	ref(s)
pristine ZnTPP		toluene	100	294	98	0:0:1	54, 56
		ethanol	77	308	<5	0:0:1	85
		E-7	100	298	98	0:0:1	54
pristine C_{60}[b]		toluene	116	−114	7	1:1:0	86
		E-7	163	−80	7	1:1:0	86
$(ZnP)_2$−Cu(I)$(phen)_2$	ZnP	toluene	170	287	88	0:0:1	this work
	ZnP	ethanol	140	280	93	0:0:1	this work
	ZnP	E-7	170	294	98	0:0:1	this work
$(ZnP)_2$−Cu(I)$(phen)_2$−C_{60}	ZnP	E-7	170	298	98	0:0:1	this work
	C_{60}	toluene	140	−84	2	1:1:0	this work
	C_{60}	ethanol	124	−93	7	1:1:0	this work
	C_{60}	E-7	170	−75	7	1:1:0	this work

[a] Uncertainty is ±5%. [b] Magnetic parameters of $^3C_{60}$* for the pristine fullerene in ethanol are unavailable.

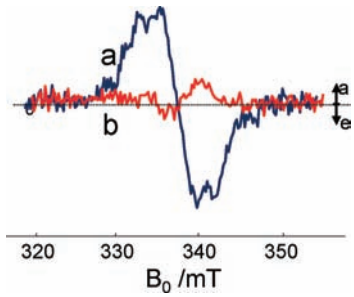

Figure 5. TREPR spectra [$\chi''(B_0)$ presentation] of $(ZnP)_2$−Cu(I)-$(phen)_2$−C_{60} in toluene at 140 K. Spectra were recorded (a) 0.3 and (b) 5.8 μs after laser-pulse photoexcitation at 460 nm.

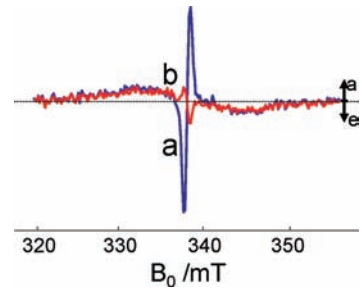

Figure 7. Time evolution of the narrow signal observed in photoexcited $(ZnP)_2$−Cu(I)$(phen)_2$−C_{60} in E-7 at 240 K. Spectra [$\chi''(B_0)$ presentation] recorded (a) 0.8 and (b) 2.0 μs after laser-pulse photoexcitation at 460 nm.

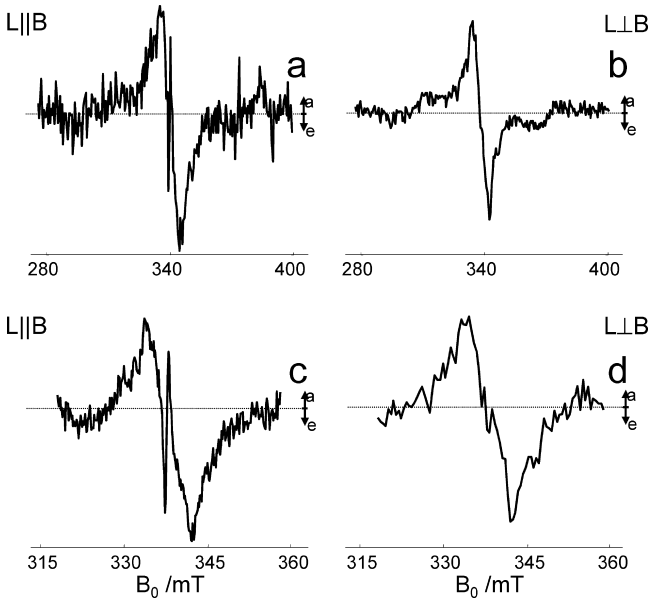

Figure 6. TREPR spectra [$\chi''(B_0)$ presentation] of $(ZnP)_2$−Cu(I)$(phen)_2$−C_{60} in E-7 at 170 K at (a,c) **L** || **B** and (b,d) **L** ⊥ **B** orientations. Spectra c and d are the expanded central parts of spectra a and b, respectively, recorded at the relevant times corresponding to the maximal signals. Spectra were recorded (a) 0.5, (b) 0.8, (c) 0.6, and (d) 1.8 μs after laser-pulse photoexcitation at 460 nm.

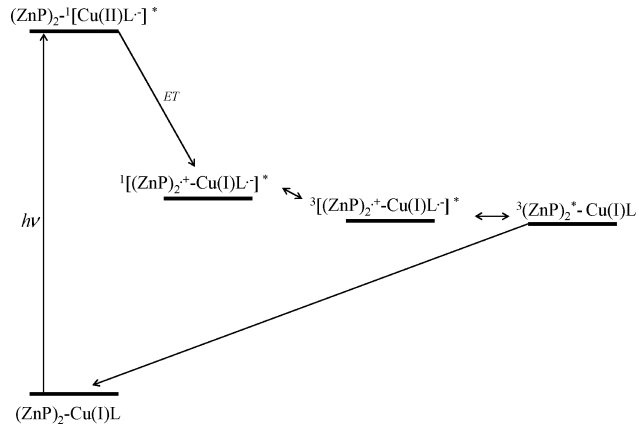

Figure 8. General presentation of the possible photoinduced processes occurring in $(ZnP)_2$−Cu(I)$(phen)_2$ in the soft crystalline and nematic phases of E-7, where L = $(phen)_2$.

of the [ZnP$^{\bullet-}$−Cu(II)$(phen)_2$] and [ZnP$^{\bullet+}$−Cu(0)$(phen)_2$] radical pairs can be ruled out on thermodynamic grounds.[25]

Based on the arguments presented above, we propose the mechanism for the SCRP formation in $(ZnP)_2$−Cu(I)$(phen)_2$ shown in Figure 8. Photoexcitation of the Cu(I)$(phen)_2$ entity forms the MLCT state in a singlet configuration, [Cu(II)−$(phen)_2^{\bullet-}$], where the electron is mostly localized on the ligand.[63] Cu(II) in this MLCT state is a powerful oxidant, which is capable of oxidizing the ZnP entity even in its ground state,[64] similarly to the reaction found in related MLCT systems.[65] As a result, the SCRP [$(ZnP)_2^{\bullet+}$−Cu(I)$(phen)_2^{\bullet-}$] is formed, accounting for the observed narrow signal.

After rapid charge separation, the correlated electron spins in the SCRP are initially in a singlet configuration. In a few nanoseconds, intersystem crossing (ISC) within the SCRP results in the formation of a relatively long-lived triplet spin configuration of the SCRP, which is observed at early times.[32,61,62] Generally, charge recombination in such an SCRP can generate a neutral triplet state of either the donor or the acceptor. In our case, the triplet of the donor (ZnP) is formed. Its decay can occur by two routes, deactivation to the ground state or thermal ET, which repopulates the RP-state-generating triplet SCRP, namely, ^{3}[$(ZnP)_2^{\bullet+}$−Cu(I)$(phen)_2^{\bullet-}$], with an a,e polarization pattern.[32,61,62] The opposite polarization pattern of the RP

spectrum at long times (~1 μs) following the laser pulse points to a triplet precursor of this RP (μ in eq 4 is positive). This mechanism is in line with the detection of the triplet-initiated SCRP only at high temperatures in the fluid phase of E-7 and with the absence of the SCRP at low temperatures in the crystalline phase of the LC. In our previous studies, we demonstrated that, contrary to charge separation, which does not depend on the solvent and is slightly affected by temperature, charge recombination is influenced by the potential barrier to solvent-dipole reorientation.[27,66] Evidently, such reorientation is facilitated in the fluid phases of LCs, where the triplet-initiated SCRP signal was observed.

Furthermore, it was shown that the dipolar interaction between the radicals in a weakly coupled SCRP is dominant and prevails over the exchange interactions.[37,38,59,60] This allows for the calculation of the spin−spin distance, r, in the SCRP using the point-dipole approximation and a $|D|$ value of 0.7 mT ($H_{pp} \approx D$). From the relation

$$D = \frac{3}{4}[(g\beta)^2/r^3] \quad (5)$$

with a g factor of 2.0041, β as the Bohr magneton, r in angstroms, and D in gauss, a value of $r \approx 16$ Å was obtained, which is in good agreement with the value calculated by HyperChem modeling ($r \approx 18$ Å). Here, r is the distance between the core metal ions in the ZnP and Cu(I)(phen)$_2$ moieties.

In a weakly coupled SCRP, the radical separation is field-dependent and proportional to $\Delta g\beta B_0$, where Δg is the difference in g factors of the radicals in the SCRP, and B_0 is the external magnetic field.[37,38,59,60] Therefore, high-field experiments (Q-band) were carried out in an attempt to separate the signals of the RP constituents. However, in these experiments, the narrow signal remained unresolved, which implies similar g values for the radicals in the SCRP. This is in line with the g values of the RP constituents, namely, 2.0025 (for ZnTPP$^{\bullet+}$)[67] and an estimated value of 2.0023 for the phenanthroline anion. The g value of the latter species is suggested to be close to that of a typical organic radical, given that the influence of the Cu(I) ion should be minor because of localization of the "transferred" electron in the MLCT on the ligand.[63]

In room-temperature optical studies of (ZnP)$_2$−Cu(I)(phen)$_2$ in DCM at 460 and 532 nm,[24−26] several EnT processes were proposed, without any indications of ET reactions. In the present work, we observed the triplet excited state of ZnP at both excitation wavelengths, in all solvents, and over a wide range of temperatures, which could be formed by direct excitation and/or via EnT from the MLCT on photoexcitation of Cu(I)(phen)$_2$. The MLCT state was not observed in our experiments, probably because of its short lifetime.[24−26] Moreover, in all phases of E-7, we could detect a singlet-initiated radical pair as a result of the photoinduced ET process from ZnP to Cu(I)(phen)$_2$ involving the MLCT (Figure 8). This process was found to occur only upon irradiation at 460 nm, where Cu(I)(phen)$_2$ absorption (with consequent MLCT formation) is significant, whereas 532-nm light, which excites mostly the ZnP entity, does not cause detectable RP formation. The lack of noticeable charge separation in the isotropic solvents, as well as efficient RP formation in E-7, are probably due to the unique properties of LCs, which stabilize the charge-separated state via relaxation of solvent dipoles.[27]

(ZnP)$_2$−Cu(I)(phen)$_2$−C$_{60}$. ***Isotropic Solvents.*** A comparison of the extinction coefficients of the ZnP, Cu(I)(phen)$_2$, and C$_{60}$ entities at both excitation wavelengths implies that a strong signal should be observed from ^{3}ZnP*, together with a weak signal for ^{3}C$_{60}$*, in frozen toluene and ethanol over a wide temperature range (as stated above, the MLCT signal could not be observed because of its short lifetime). However, all samples exhibited a very weak signal for ^{3}ZnP*, suggesting efficient quenching of the photoexcited porphyrin by the other entities, as found in the optical experiments.[24−26] In addition, two narrower signals were observed under these conditions. The magnetic parameters of the wider signal allow its attribution to the lowest triplet state of C$_{60}$ (Table 1), originating from the direct excitation of the C$_{60}$ entity

$$C_{60} \xrightarrow{h\nu} {}^1C_{60}^* \xrightarrow{\text{ISC}} {}^3C_{60}^*$$

and/or through EnT from the excited ZnP[50,68,69]

$$ZnP \xrightarrow{h\nu} {}^1ZnP^* \xrightarrow{\text{EnT}} {}^3C_{60}^*$$

Additionally, we cannot rule out ^{3}C$_{60}$* formation through EnT from the MLCT state. As to the narrower signal, based on its kinetic and magnetic parameters, we ascribe it to a charge-separated state,[70−73] which generally can be formed through two possible pathways, namely, the TRP and SCRP mechanisms.

We exclude ET reactions between the (ZnP)$_2$ and C$_{60}$, as well as between (ZnP)$_2$ and Cu(I)(phen)$_2$ in (ZnP)$_2$−Cu(I)(phen)$_2$−C$_{60}$ via both these mechanisms, because the moieties are separated by ~31 and ~18 Å, respectively. The former distance is that between the center of the porphyrin and the adjacent "surface" of the fullerene molecule where the excited electron is localized on the C$_{60}$ "equator".[74] It is well-established that exchange interactions between two spins separated by such distances are negligibly small.[75] Thus, the simlar g values of the constituents in these RPs imply the presence of one unresolved multiplet line in their spectra, with a width governed only by the dipolar interactions. For such distances, the point-dipole approximation (eq 5) gives values for the ZFS parameter $|D|$ of 0.09 and 0.5 mT, respectively, which are quite far from the D value of the observed signal ($H_{pp} \approx 4.2$ mT). A further feasible ET process can occur in the Cu(I)(phen)$_2$−C$_{60}$ pair where the distance between the constituents is ~13 Å (here, the distance is defined as that between the copper ion and the equator of the fullerene sphere).[74] Generally, at such distances, both dipole and exchange interactions are operative and contribute to broaden the RP spectral width to the observed value. However, in this case, we can eliminate TRP formation mainly because the TRP spectrum should be centered about the mean value of the g factors of the RP's constituents, namely, 2.0650, which is the average of the values of Cu(II)(phen)$_2$ ($g_{iso} \approx 2.13$)[76] and C$_{60}^{\bullet-}$ ($g \approx 1.9999$).[77] Clearly, this is not the case, given that the experimentally determined g factor of the RP is significantly smaller (~2.0030).

Analyzing the parameters of the charge-separated state (see below), we attributed the narrowest observed signal to the weakly coupled SCRP formed by the photoinduced ET reaction

$$Cu(I)(phen)_2{-}C_{60} \xrightarrow{h\nu} Cu(II)(phen)_2{-}C_{60}^{\bullet-}$$

(Here, we do not consider ET in the opposite direction, as it is considerably less thermodynamically feasible.)[9−11,24,46]

The constituents of the Cu(II)(phen)$_2$−C$_{60}^{\bullet-}$ pair are characterized by very distinct g values, namely, $g_{iso} \approx 2.13$ for Cu(II)(phen)$_2$[76] and $g \approx 1.9999$ for C$_{60}^{\bullet-}$.[77] Therefore, in our

experiments, the magnetic field should efficiently separate these signals.[78] We believe that this is indeed the case. However, we must take into account the fact that the EPR spectrum of Cu(II)(phen)$_2$ is much broader than that of $C_{60}^{\bullet-}$ (~94[76] vs ~1.1[77] mT). Thus, the amplitude of the Cu(II)(phen)$_2$ signal is expected to be dramatically lower than that of $C_{60}^{\bullet-}$. Moreover, for complexes containing a Cu(II) ion and a stable organic radical, it was shown that intramolecular electron exchange between these species noticeably broadens their EPR spectra.[79,80] Suggesting the occurrence of this effect in Cu(II)(phen)$_2$−$C_{60}^{\bullet-}$, one can assess its magnitude by the example of $C_{60}^{\bullet-}$, whose parameter H_{pp} of 0.55 mT[77] is increased to 4.2 mT as was observed in our experiments. Thus, the exchange interaction in our system should mainly contribute to the line width of the observed signal; that is, the J value is expected to be several millitesla, which is reasonable at such distances (~13 Å)[81−83] (vs $|D| \approx 1.2$ mT as calculated from the point-dipole approximation).

Estimation of the parameter Q (eq 3) shows that it is significantly larger than $|J|$, which is in line with our suggestion of a weak spin coupling in Cu(II)(phen)$_2$−$C_{60}^{\bullet-}$ pair.[37,38,40,76,77]

Because the g value of the observed narrow signal is around 2.00, we assign it to the $C_{60}^{\bullet-}$ part of the RP, whereas the much weaker signal of Cu(II)(phen)$_2$ is masked by that of the ^{3}ZnP*. Assuming a positive sign for the exchange integral J, one can consider the photoexcited singlet state of MLCT as the precursor of the charge separation (eq 4). Furthermore, we explain the inversion of the initial a,e polarization pattern of the narrow signal to e,a at later times (Figure 5) by RP formation occurring via two routes, namely, from singlet and from triplet precursors.[39] We emphasize here that, in (ZnP)$_2$−Cu(I)(phen)$_2$−C_{60} in DCM at room temperature, the two charge-separated states (ZnP)$_2$−Cu(II)(phen)$_2$−$C_{60}^{\bullet-}$ and (ZnP)$_2^{\bullet+}$−Cu(I)(phen)$_2$−$C_{60}^{\bullet-}$ were suggested to be in equilibrium.[25] Our observation that only (ZnP)$_2$−Cu(II)(phen)$_2$−$C_{60}^{\bullet-}$ is formed in toluene and ethanol at low temperatures can be explained by a shift of the equilibrium resulting from the drastic change in the experimental conditions.

It should also be noted here that the lack of an RP signal in the glass phase of toluene, where the motion of the rotaxane parts is hampered, points to a crucial role of supramolecular conformational factors in "tuning" the efficiency of ET processes. Indeed, the changes in the physical properties of the solvent upon freezing should also contribute to the effect accordingly.

Liquid Crystal. Comparison of the TREPR spectra obtained upon photoexcitation of (ZnP)$_2$−Cu(I)(phen)$_2$ and (ZnP)$_2$−Cu(I)(phen)$_2$−C_{60} shows a number of similarities in their magnetic and kinetic parameters. More specifically, the broad a,e spectra (~70 mT width) obtained at 460 and 532 nm are assigned in both cases to ^{3}ZnP*. The practically identical narrow signals ($H_{pp} \approx 0.7$ mT) in both rotaxanes observed only upon 460-nm excitation are ascribed to the same singlet-initiated SCRP, namely (ZnP$^{\bullet+}$)$_2$-Cu(I)(phen)$_2^{\bullet-}$. All features of the narrow signal found in (ZnP)$_2$−Cu(I)(phen)$_2$−C_{60} can be explained in a manner similar to that used for the corresponding signal found in (ZnP)$_2$−Cu(I)(phen)$_2$ (Figure 9). On the other hand, we should point out the sole difference in ET processes occurring in (ZnP)$_2$−Cu(I)(phen)$_2$ and (ZnP)$_2$−Cu(I)(phen)$_2$−C_{60}, namely, that 460-nm excitation of the former rotaxane at low temperatures (113 and 120 K) does not result in a detectable RP, whereas in the latter system, a well-resolved RP signal is observed down to 120 K.

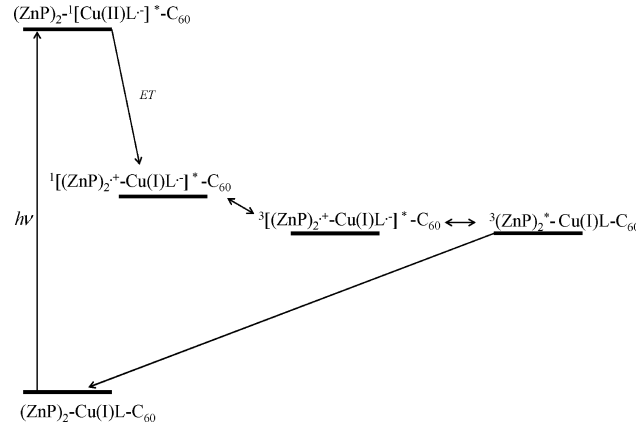

Figure 9. General presentation of the possible photoinduced processes occurring in (ZnP)$_2$−Cu(I)(phen)$_2$−C_{60} in the soft crystalline and nematic phases of E-7, where L = (phen)$_2$.

Line-shape analysis of the 20 mT width signal observed with (ZnP)$_2$−Cu(I)(phen)$_2$−C_{60} allows its attribution to $^3C_{60}$*. Inspection of the spectra shows that, despite the low probability of light absorption by C_{60}, as compared to that of ZnP, the $^3C_{60}$* signal intensity is high. This points to efficient EnT from ^{1}ZnP* to C_{60} (via the MLCT state) taking place in the photoexcited system under these conditions. In DCM solution, using optical methods, exergonic EnT from ^{1}ZnP* to the MLCT state of the Cu(I) complex was observed, which led to the long-range charge-separated state (ZnP)$_2^{+\bullet}$-Cu(I)(phen)$_2$−$C_{60}^{-\bullet}$,[25,26] for which no evidence was found in the present TREPR studies.

Finally, we discuss the differences in the behavior of photoexcited (ZnP)$_2$−Cu(I)(phen)$_2$ and (ZnP)$_2$−Cu(I)(phen)$_2$−C_{60} systems found in the present TREPR investigation and previous optical studies. Here, it must be emphasized that the TREPR experiments were carried out in frozen toluene and ethanol as well as in the crystalline, soft crystalline, and nematic phases of LC, whereas the optical studies were performed in DCM at room temperature.

It is well-established that a large number of factors affect photoinduced ET dynamics, including donor−acceptor electronic coupling, free energy change, and total reorganization energy, all of which strongly depend on the solvent properties. More specifically, in terms of Marcus theory, the rate constant for electron transfer, k_{ET}, is given by[84]

$$k_{ET} = \frac{2\pi}{\hbar}|V|^2(\mathrm{FC})$$

where V is the matrix element of coupling between the initial and final electronic states and FC is the average nuclear Franck−Condon factor. The former term depends on the donor−acceptor distance and mutual orientation, whereas the latter is a function of the free energy of charge separation and the total solvent reorganization energy. Indeed, both V and FC directly or indirectly are temperature-dependent. In turn, the total reorganization energy can be separated into the inner-sphere and outer-sphere reorganization energies. These terms refer to the energy changes accompanying changes in the bond length and bond angles during the ET step and to the energy changes of reorganization of the solvent shells surrounding the reactants, respectively. Thus, solvent properties strongly affect both the reaction free energy and its net activation barrier.[27,42,50,61,68,69] We believe that, in the case of our large rotaxane supramolecules, which have significant conformational mobility because of rotation around the bonds of the polyether linkers in the thread, the combined solvent effects will govern the main

parameters of the light-driven photophysical and photochemical reactions.

Conclusions

In summary, we have demonstrated that the efficiencies and routes of the photoinduced ET and EnT processes in rotaxanes are strongly dependent on the properties of their microenvironment. Comparison of the data presented in this paper with the optical spectroscopy results obtained earlier,[25,26] shows that the relaxation of the photoexcited entities in $(ZnP)_2-Cu(I)(phen)_2$ and $(ZnP)_2-Cu(I)(phen)_2-C_{60}$ occurs differently in glassy, amorphous, and liquid states of isotropic solvents, as well as in the crystalline and nematic phases of LCs. We attribute these findings to the relatively high conformational mobility of the mechanically interlocked rotaxane systems, enabling conformational changes to take place depending on the precise microenvironment properties and the temperature. These changes in rotaxane conformation coupled with variations in the solvent properties can modify the thermodynamic parameters of the relevant ET reactions, which will significantly affect the pathways and dynamics upon relaxation of the electronic excited states. It would be of interest in this connection to compare the behavior at low temperatures of the conformationally flexible rotaxane $(ZnP)_2-Cu(I)(phen)_2-C_{60}$ with that of the more rigid catenane in which the two ZnP moieties are linked with a bidentate ligand such as 4,4′-bipyridine.[24]

Hence, revealing a structure−medium−function correlation in rotaxanes such as these might serve as a basis for the fine-tuning of light-driven processes in the various applications of these interesting systems.

Acknowledgment. The work at HUJ was supported by the Israel Science Foundation (Grant 740/06), Deutsche Forschungsgemeinschaft, and the KAMEA foundation (A.B.). This work is in partial fulfillment of the requirements for a Ph.D. degree (M.J.) at HUJ. The work at NYU was supported by grants from the National Science Foundation, the Petroleum Research Fund of the American Chemical Society, and the Research Challenge Fund of New York University. We are grateful to Prof. G. Kothe and Mr. T. Berthold (University of Freiburg, Freiburg, Germany) for carrying out control Q-band experiments and to Dr. E. Stavitski for his help in running some experiments.

References and Notes

(1) Chance, B.; Nishimura, M. *Proc. Natl. Acad. Sci. U.S.A.* **1960**, *46*, 19.

(2) Sundstrom, V. Photosynthetic light harvesting, charge separation, and photoprotection: The primary steps. In *Photobiology: The Science of Life and Light*, 2nd ed.; Bjorn, L. O., Ed.; Springer: New York, 2008; p 289.

(3) Levanon, H.; Möbius, K. *Annu. Rev. Biophys. Biomol. Sci.* **1997**, *26*, 495.

(4) LaVan, D. A.; Cha, J. N. *Proc. Natl. Acad. Sci. U.S.A.* **2006**, *103*, 5251.

(5) Bravo, J. A.; Raymo, F. M.; Stoddart, J. F.; White, A. J. P.; Williams, D. J. *Eur. J. Org. Chem.* **1998**, *1998*, 2565.

(6) Brouwer, A. M.; Fazio, S. M.; Frochot, C.; Gatti, F. G.; Leigh, D. A.; Wong, J. K. Y.; Wurpel, G. W. H. *Pure Appl. Chem.* **2003**, *75*, 1055.

(7) Stowell, M. H. B.; McPhillips, T. M. *Science* **1997**, *276*, 812.

(8) Darrouzet, E.; Valkova-Valchanova, M.; Moser, C. C.; Dutton, P. L.; Daldal, F. *Proc. Natl. Acad. Sci. U.S.A.* **2000**, *97*, 4567.

(9) El-Khouly, M. E.; Ito, O.; Smith, P. M.; D'Souza, F. *J. Photochem. Photobiol. C: Photochem. Rev.* **2004**, *5*, 79.

(10) Sandanayaka, A. S. D.; Watanabe, N.; Ikeshita, K. I.; Araki, Y.; Kihara, N.; Furusho, Y.; Ito, O.; Takata, T. *J. Phys. Chem. B* **2005**, *109*, 2516.

(11) Mateo-Alonso, A.; Ehli, C.; Rahman, G. M. A.; Guldi, D. M.; Fioravanti, G.; Marcaccio, M.; Paolucci, F.; Prato, M. *Angew. Chem., Int. Ed.* **2007**, *46*, 3521.

(12) Flamigni, L.; Armaroli, N.; Barigelletti, F.; Chambron, J.-C.; Sauvage, J.-P.; Solladie, N. *New J. Chem.* **1999**, *23*, 1151.

(13) Sauvage, J.-P. *Acc. Chem. Res.* **1998**, *31*, 611.

(14) Chambron, J.-C.; Collin, J.-P.; Dalbavie, J.-O.; Dietrich-Buchecker, C. O.; Heitz, V.; Odobel, F.; Solladie, N.; Sauvage, J.-P. *Coord. Chem. Rev.* **1998**, *178*, 1299.

(15) Benniston, A. C.; Harriman, A. *Angew. Chem., Int. Ed.* **1993**, *32*, 1459.

(16) Vale, R. D.; Milligan, R. A. *Science* **2000**, *288*, 88.

(17) Bustamante, C.; Chemla, Y. R.; Forde, N. R.; Izhaky, D. *Annu. Rev. Biochem.* **2004**, *73*, 705.

(18) Balzani, V.; Clemente-Leon, M.; Credi, A.; Ferrer, B.; Venturi, M.; Flood, A. H.; Stoddart, J. F. *Proc. Natl. Acad. Sci.USA* **2006**, *103*, 1178.

(19) Willner, I.; Basnar, B.; Willner, B. *Adv. Funct. Mater.* **2007**, *17*, 702.

(20) Baranoff, E.; Barigelletti, F.; Bonnet, S.; Collin, J.-P.; Flamigni, L.; Mobian, P.; Sauvage, J.-P. *Struct. Bonding (Berlin)* **2007**, *123*, 41.

(21) Ballardini, R.; Balzani, V.; Credi, A.; Gandolfi, M. T.; Venturi, M. *Acc. Chem. Res.* **2001**, *34*, 445.

(22) Andersson, M.; Linke, M.; Chambron, J.-C.; Davidsson, J.; Heitz, V.; Hammarstrom, L.; Sauvage, J.-P. *J. Am. Chem. Soc.* **2002**, *124*, 4347.

(23) Sandanayaka, A. S. D.; Sasabe, H.; Araki, Y.; Furusho, Y.; Ito, O.; Takata, T. *J. Phys. Chem. A* **2004**, *108*, 5145.

(24) Schuster, D. I.; Li, K.; Guldi, D.; Ramey, J. *Org. Lett.* **2004**, *6*, 1919.

(25) Li, K.; Schuster, D. I.; Guldi, D. M.; Herranz, M. A.; Echegoyen, L. *J. Am. Chem. Soc.* **2004**, *126*, 3388.

(26) (a) Schuster, D. I.; Li, K.; Guldi, D. M. *C. R. Chim.* **2006**, *9*, 892. (b) Li, K. Ph.D. Dissertation, New York University, New York, 2004.

(27) Levanon, H.; Hasharoni, K. *Prog. React. Kinet.* **1995**, *20*, 309.

(28) Collin, J.-P.; Dietrich-Buchecker, C.; Gavina, P.; Jimenez-Molero, M.; Sauvage, J.-P. *Acc. Chem. Res.* **2001**, *34*, 447.

(29) Berna, J.; Leigh, D. A.; Lubomska, M.; Mendoza, S. M.; Perez, E. M.; Rudolf, P.; Teobaldi, G.; Zerbetto, F. *Nat. Mater.* **2005**, *4*, 704.

(30) Guldi, D. M.; Rahman, A.; Sgobba, V.; Ehli, C. *Chem. Soc. Rev.* **2006**, *35*, 471.

(31) Saha, S.; Flood, A. H.; Stoddart, J. F.; Impellizzeri, S.; Silvi, S.; Venturi, M.; Credi, A. *J. Am. Chem. Soc.* **2007**, *129*, 12159.

(32) Jakob, M.; Berg, A.; Stavitski, E.; Chernick, E. T.; Weiss, E. A.; Wasielewski, M. R.; Levanon, H. *Chem. Phys.* **2006**, *324*, 63.

(33) Wagnert, L.; Berg, A.; Stavitski, E.; Berthold, T.; Kothe, G.; Goldberg, I.; Mahammed, A.; Simkhovich, L.; Gross, Z.; Levanon, H. *Appl. Magn. Reson.* **2006**, *30*, 591.

(34) Regev, A.; Galili, T.; Levanon, H. *J. Chem. Phys.* **1991**, *95*, 7907.

(35) Gonen, O.; Levanon, H. *J. Phys. Chem.* **1984**, *88*, 4223.

(36) Blank, A.; Levanon, H. *Concepts Magn. Reson. A* **2005**, *25*, 18.

(37) Hore, P. J. In *Advanced EPR Applications in Biology and Biochemistry*; Hoff, A. J., Ed.; Elsevier: Amsterdam, 1989; p 405.

(38) Efimova, O.; Hore, P. J. *Biophys. J.* **2008**, *94*, 1565.

(39) Salikhov, K. M.; Molin, Y. N.; Segdeev, R. Z.; Buchachenko, A. L. *Spin Polarization and Magnetic Effects in Radical Reactions*; Elsevier: Amsterdam, 1984.

(40) Norris, J. R.; Morris, A. L.; Thurnauer, M. C.; Tang, J. *J. Chem. Phys.* **1990**, *92*, 4239.

(41) Furrer, R.; Fujara, F.; Lange, C.; Stehlik, D.; Vieth, H. M.; Vollmann, W. *Chem. Phys. Lett.* **1980**, *75*, 332.

(42) Kavarnos, G. J. *Fundamentals of Photoinduced Electron Transfer*; VCH Publishers, Inc.: New York, 1993.

(43) Bialkowski, S. E. Parameters for Common Solvents Used in Photothermal and Photoacoustic Spectrometry. Utah State University, Logan, UT; available at http://www.chem.usu.edu/~sbialkow/Research/Tablevalues.html (accessed November 2008).

(44) Merck Ltd. Catalog: Nematic Liquid Crystal Mixtures; E-Merck Ltd.: Mumbai, India, 1989.

(45) Unfortunately, we could not carry out TREPR experiments under the same experimental conditions, in DCM at room temperature, as performed in the recent optical studies.[24−26] This solvent does not form a glass at low temperatures, whereas in the liquid state, significant dielectric losses do not permit TREPR measurements to be performed with our experimental setup.

(46) Ruthkosky, M.; Kelly, C. A.; Castellano, F. N.; Meyer, G. J. *Coord. Chem. Rev.* **1998**, *171*, 309.

(47) *Optical Spectra*; Oregon Medical Laser Center, Portland, OR; available at http://omlc.ogi.edu/spectra/PhotochemCAD/abs_html/ZnTPP.html. (accessed November 2008).

(48) Moravsky, A. P.; Fursikov, P. V.; Kachapina, L. M.; Khramov, A. V.; Kiryakov, N. V. UV-VIS Photometric Analysis of Fullerenes C_{60} and C_{70} in Toluene and Hexane Solutions. In *Recent Advances in the*

Chemistry and Physics of Fullerenes; Ruoff, R. S., Kadish, K. M., Eds.; The Electrochemical Society: Pennington, NJ, 1995; Vol. 2; p 156.

(49) The presented extinction coefficients and excited-state energies were taken for the pristine compounds: ZnTPP, $Cu(I)(phen)_2$, and C_{60}. We suggest that, for the mechanically interlocked supramolecular moieties, these values should be close to the corresponding ones in the rotaxanes studied here.

(50) Galili, T.; Regev, A.; Levanon, H.; Schuster, D. I.; Guldi, D. M. *J. Phys. Chem. A* **2004**, *108*, 10632.

(51) Parker, W. L.; Crosby, G. A. *J. Phys. Chem.* **1989**, *93*, 5692.

(52) Kirchhoff, J. R.; Gamache, R. E.; Blaskie, M. W.; Del Paggio, A. A.; Lengel, R. K.; McMillin, D. R. *Inorg. Chem.* **1983**, *22*, 2380.

(53) Regev, A.; Levanon, H.; Murai, T.; Sessler, J. L. *J. Chem. Phys.* **1990**, *92*, 4718.

(54) Gonen, O.; Levanon, H. *J. Phys. Chem.* **1985**, *89*, 1637.

(55) Gouterman, M.; Yamanishi, B. S.; Kwiram, A. L. *J. Chem. Phys.* **1972**, *56*, 4073.

(56) Scherz, A.; Levanon, H. *J. Phys. Chem.* **1980**, *84*, 324.

(57) Alba, C.; Busse, L. E.; List, D. J.; Angell, C. A. *J. Chem. Phys.* **1990**, *92*, 617.

(58) Haida, O.; Suga, H.; Seki, S. *J. Chem. Thermodyn.* **1977**, *9*, 1133.

(59) Closs, G. L.; Forbes, M. D. E.; Norris, J. R. *J. Phys. Chem.* **1987**, *91*, 3592.

(60) Norris, J. R.; Morris, A. L.; Thurnauer, M. C.; Tang, J. *J. Chem. Phys.* **1990**, *92*, 4239.

(61) Hasharoni, K.; Levanon, H.; Greenfield, S. R.; Gosztola, D. J.; Svec, W. A.; Wasielewski, M. R. *J. Am. Chem. Soc.* **1996**, *118*, 10228.

(62) Shaakov, S.; Galili, T.; Stavitski, E.; Levanon, H.; Lukas, A.; Wasielewski, M. R. *J. Am. Chem. Soc.* **2003**, *125*, 6563.

(63) Gordon, K. C. J.; McGarvey, J. J. *Inorg. Chem.* **1991**, *30*, 2986.

(64) Flamigni, L. *Pure Appl. Chem.* **2001**, *73*, 241.

(65) Schanze, K. S.; Walters, K. A. Photoinduced Electron Transfer in Metal−Organic Dyads. In *Organic and Inorganic Photochemistry*; Molecular and Supramolecular Photochemistry Series; Marcel Dekker: New York, 1998; Vol. 2, p 75.

(66) Hasharoni, K.; Levanon, H.; Gätschmann, J.; Schubert, H.; Kurreck, H.; Möbius, K. *J. Phys. Chem.* **1995**, *99*, 7514.

(67) Felton, R. H. Redox Reactions of Metalloporphyrins. In *The Porphyrins*; Dolphin, D., Ed.; Academic Press: New York, 1978; Vol. 5, p 53.

(68) Galili, T.; Regev, A.; Berg, A.; Levanon, H.; Schuster, D. I.; Möbius, K.; Savitsky, A. *J. Phys. Chem. A* **2005**, *109*, 8451.

(69) Regev, A.; Galili, T.; Levanon, H.; Schuster, D. I. *J. Phys. Chem. A* **2006**, 110.

(70) Hasharoni, K.; Levanon, H.; Tang, J.; Bowman, M. K.; Norris, J. R.; Gust, D.; Moore, T. A.; Moore, A. L. *J. Am. Chem. Soc.* **1990**, *112*, 6477.

(71) Levanon, H.; Bowman, M. K. *Time-Domain EPR Spectroscopy of Energy and Electron Transfer*; Academic Press: New York, 1993.

(72) Hasharoni, K.; Levanon, H.; von Gersdorff, J.; Kurreck, H.; Möbius, K. *J. Chem. Phys.* **1993**, *98*, 2916.

(73) Levanon, H.; Galili, T.; Regev, A.; Wiederrecht, G. P.; Svec, W.; Wasielewski, M. R. *J. Am. Chem. Soc.* **1998**, *120*, 6366.

(74) Visser, J.; Groenen, E. J. J. *Chem. Phys. Lett.* **2002**, *356*, 43.

(75) Molin, Y. N.; Salikhov, K. M.; Zamaraev, K. I. *Spin Exchange, Principles and Applications in Chemistry and Biology*; Springer: New York, 1980.

(76) Ferrer, E. G.; Tévez, L. L. L.; Baeza, N.; Correa, M. J.; Okulik, N.; Lezama, L.; Rojo, T.; Castellano, E. E.; Piro, O. E.; Williams, P. A. M. *J. Inorg. Biochem.* **2007**, *101*, 741.

(77) Dubois, D.; Jones, M. T.; Kadish, K. M. *J. Am. Chem. Soc.* **1992**, *114*, 6446.

(78) Berg, A.; Shuali, Z.; Asano-Someda, M.; Levanon, H.; Fuhs, M.; Möbius, K.; Wang, R.; Sessler, J. L. *J. Am. Chem. Soc.* **1999**, *121*, 7433.

(79) Sawant, B. M.; Braden, G. A.; Smith, R. E.; Eaton, G. R.; Eaton, S. S. *Inorg. Chem.* **1981**, *20*, 3349.

(80) Ahn, W. S.; Zhong, Y. P.; Lim, P. K. *Korean J. Chem. Eng.* **1997**, *14*, 394.

(81) Okamura, M. Y.; Isaacson, R. A.; Feher, G. *Biochim. Biophys. Acta* **1979**, *546*, 394.

(82) Hoffmann, S. K.; Hilczer, W.; Goslar, J. *Appl. Magn. Reson.* **1994**, *7*, 289.

(83) Mazzoni, M.; Franco, L.; Corvaja, C.; Zordan, G.; Menna, E.; Scorrano, G.; Maggini, M. *ChemPhysChem* **2002**, 527.

(84) Marcus, R. A. *Annu. Rev. Phys. Chem.* **1964**, *15*, 155.

(85) *The Porphyrins*; Dolphin, D., Ed.; Academic Press Inc.: London, 1979; Vol. 4, p 278.

(86) Regev, A.; Gamliel, D.; Meiklyar, V.; Michaeli, S.; Levanon, H. *J. Phys. Chem.* **1993**, *97*, 3671.

JP900331J